University of Sistan and Baluchestan

Journal of Epigenetics

Online ISSN: 2676 - 4350

Homepage: https://jep.usb.ac.ir

Iranian Genetics Society

Botanical disruption of host-pathogen interactions and biofilm gene expression in uropathogenic Klebsiella pneumoniae

Ali Qasemi [1*]

[1] *Corresponding author*, Dept. of Biology, Faculty of Science, University of Sistan and Baluchestan, Zahedan, Iran. E-mail: Qasemi@science.usb.ac.ir.

ARTICLE INFO

Article type:
Research Article

Article history:
Received:21 January 2026
Revised:18 February 2026
Accepted:6 March 2026

Keywords:
Klebsiella pneumoniae,
Biofilm inhibition,
Botanical Extracts,
Anti-virulence therapy,
Host-pathogen interaction,
Gene expression.

A B S T R A C T

The increasing prevalence of biofilm-forming Klebsiella pneumoniae in urinary tract infections (UTIs) necessitates the exploration of alternative plant-based therapeutics. This study aimed to comparatively evaluate the anti-biofilm and virulence-attenuating properties of aqueous extracts from Mesembryanthemum nodiflorum (ice plant) and Maclura pomifera (Osage orange) against clinical K. pneumoniae isolates. Clinically confirmed K. pneumoniae isolates were screened for biofilm formation capacity. Following the preparation of both plant extracts, their minimum inhibitory concentrations (MICs) were determined. Furthermore, the sub-inhibitory impacts of these extracts on biofilm formation, bacterial adhesion, and invasion in the human epithelial cell model (HK-2) were evaluated. The transcriptional modulation of key virulence genes (fimH, mrkA, rmpA, wzi, luxS) was assessed using qRT-PCR. Cytotoxicity was evaluated via the MTT assay. Among the isolates, 80.9% exhibited biofilm-producing capabilities. The M. nodiflorum extract demonstrated a superior inhibitory profile (MIC = 256 µg/mL) compared to M. pomifera (MIC = 512 µg/mL). At sub-MIC levels, M. nodiflorum significantly reduced biofilm biomass by 41.7%, whereas M. pomifera achieved only a 22.5% reduction. Similarly, host cell adhesion and intracellular invasion were suppressed by approximately 45% using M. nodiflorum, compared to a marginal 20–24% reduction by M. pomifera. Transcriptional profiling confirmed that M. nodiflorum strongly downregulated fimH, mrkA, rmpA, wzi, and luxS expression, while the regulatory impact of M. pomifera was notably weaker. Both extracts maintained high host cell viability (>89%) at therapeutic doses. The M. nodiflorum aqueous extract exhibits significantly higher translational potential than M. pomifera as an anti-virulence agent. By effectively disrupting the biofilm genetic architecture and limiting host-pathogen interactions, M. nodiflorum offers a promising scaffold for managing K. pneumoniae-associated UTIs

Introduction

The clinical management of urinary tract infections (UTIs) is currently facing a severe bottleneck, largely driven by the adaptive resilience of *Klebsiella pneumoniae* (Timm et al., 2025). As an opportunistic pathogen, it frequently colonizes the urinary tract and aggressively complicates treatment regimens. The true survival advantage of this bacterium lies in its sophisticated biofilm architecture, which acts as a physical barrier, restricting therapeutic penetration and shielding the bacterial community from host immune responses (Mim et al., 2026).

DOI: https://doi.org/ 10.22111/jep.2026.55683.1110

 Publisher: University of Sistan and Baluchestan

How to Cite: Qasemi, A.(2026). Botanical disruption of host-pathogen interactions and biofilm gene expression in uropathogenic Klebsiella pneumoniae. *Journal of Epigenetics*, 7(1), 64-71. https://doi.org/ 10.22111/jep.2026.55683.1110

The transition into this recalcitrant state is not a random event; it is strictly orchestrated by a network of specific virulence genes. Fimbrial adhesins, primarily encoded by the *fimH* (type 1 fimbriae) and *mrkA* (type 3 fimbriae) genes, act as the critical molecular hooks that facilitate the initial docking to host tissues. Following attachment, the *rmpA* gene operates as a master regulator to drive the hypermucoviscous phenotype, while *wzi* is essential for the surface assembly of the capsular polysaccharide. Concurrently, the *luxS* gene drives the quorum-sensing communication required for biofilm maturation (Abhinand et al., 2025; Dong et al., 2022).

Attempting to eradicate these mature, genetically fortified biofilms with conventional bactericidal drugs often proves ineffective. Consequently, contemporary microbiological research is pivoting toward anti-virulence strategies. Rather than simply aiming to kill the pathogen, dismantling its genetic infrastructure and disarming its invasive capabilities offers a much smarter therapeutic approach (Ding et al., 2025).

Botanical extracts, characterized by their diverse phytochemical matrices, are emerging as prime candidates for this strategy. *Mesembryanthemum nodiflorum* (ice plant) has drawn particular interest due to its robust internal reservoir of bioactive flavonoids (Arena et al., 2020). Similarly, *Maclura pomifera* (Osage orange) is rich in prenylated isoflavones and phenolic acids (Sainz-Hernández et al., 2023). While the general antibacterial traits of these two plants have been explored individually, a direct, mechanistic comparison of their anti-virulence efficacies against uropathogenic *K. pneumoniae* remains absent.

Therefore, the present study was designed to comparatively evaluate the therapeutic potential of *M. nodiflorum* and *M. pomifera* aqueous extracts. We aimed to quantify their capacity to eradicate established biofilms, investigate their protective effects against bacterial invasion in human epithelial models, and trace these phenotypic outcomes directly to the transcriptional modulation of the *fimH*, *mrkA*, *rmpA*, *wzi*, and *luxS* virulence network.

Materials and Methods

Bacterial Isolation and Identification

Clinical urine specimens were collected from patients experiencing symptomatic urinary tract infections. Presumptive *K. pneumoniae* colonies were identified through a standard biochemical series, and their exact identity was confirmed at the molecular level by amplifying the species-specific 16S rRNA gene (Moses et al., 2024). Specifically, these isolates were previously characterized as multidrug-resistant (MDR) and extended-spectrum beta-lactamase (ESBL) producers according to standard phenotypic screening. Verified isolates were frozen in 20% glycerol at -20°C for subsequent testing.

Determination of Biofilm-Forming Ability

We assessed the biofilm-forming capacity of the clinical isolates using a standard 96-well microtiter plate crystal violet (CV) approach (Thibeaux et al., 2020). Overnight bacterial cultures adjusted to a 0.5 McFarland standard were diluted (1:100) into fresh Luria-Bertani (LB) broth. From this mixture, 200 µL aliquots were seeded into flat-bottom polystyrene plates and incubated at 37°C for 24 hours. After removing non-adherent cells and washing with PBS (pH 7.4), the remaining biomass was stained with 0.1% crystal violet for 15 minutes. The bound dye was dissolved using 95% ethanol, and the optical density was recorded at 570 nm to categorize the isolates from non-producers to strong biofilm producers (Stepanović et al., 2007).

Minimum Inhibitory Concentration (MIC) Determination

The aqueous extracts were prepared via standard maceration. Briefly, 50 g of dried plant powder was soaked in 500 mL of sterile distilled water for 48 hours at room temperature, filtered, and subsequently freeze-dried, yielding an approximate extraction efficiency of 12% and 15% for *M. nodiflorum* and *M. pomifera*, respectively. To measure the baseline inhibitory thresholds of both botanical extracts, we utilized broth microdilution assays (CLSI, 2021). A well-characterized reference strain (*K. pneumoniae* ATCC 700603) and our most robust clinical isolate were exposed to serial dilutions of the extracts. Ciprofloxacin (10 µg/mL) was included as a standard positive control to establish a comparative baseline. The MIC was recorded as the lowest concentration that completely blocked visible bacterial growth.

Targeted Antibiofilm Assay at Sub-Inhibitory Concentrations

To evaluate true anti-virulence activity without inducing growth-inhibition artifacts, biofilm eradication assays were conducted at strictly sub-inhibitory doses (half of the MIC, ½ MIC). Standardized bacterial suspensions were incubated in 96-well plates containing the plant extracts at these levels. After 24 hours at 37°C, the surviving adherent biomass was stained with crystal violet and quantified at 570 nm (Haney et al., 2018). To confirm that the biomass reduction was associated with decreased cellular viability rather than mere matrix disruption, a supplementary Resazurin metabolic assay was performed alongside the CV assay.

Host Cell-Pathogen Interaction Assays

Human kidney proximal tubular epithelial cells (HK-2) were cultured in DMEM enriched with 10% fetal bovine serum. Confluent monolayers were challenged with *K. pneumoniae* at a multiplicity of infection (MOI) of 10:1, either leaving them untreated or exposing them to the plant extracts at ½ MIC. To measure bacterial adhesion, co-cultures were incubated for 2 hours. This specific timeframe was selected based on previously optimized kinetic models for *K. pneumoniae* adhesion, capturing peak docking without significant bacterial replication. Following this, cells were washed and lysed with 0.1% Triton X-100 to count the attached CFUs. For the invasion assay, a parallel set of infected cells was treated with gentamicin (100 µg/mL) for an additional 2 hours to eliminate extracellular bacteria before lysis and plating (Rana et al., 2025). A preliminary checkerboard assay confirmed that the plant extracts at ½ MIC do not exhibit synergistic or antagonistic interactions with Gentamicin.

In Vitro Cytotoxicity Assessment

The cytocompatibility of both extracts was evaluated using a standard MTT assay on the HK-2 cell line (Ghasemi et al., 2023). Epithelial cells were exposed to the respective ½ MIC doses of the extracts for 24 hours. By measuring the metabolic activity of the treated cells compared to healthy untreated controls. The final concentration of DMSO (used as the primary solvent) in the treated wells never exceeded 0.1% (v/v), and a 0.1% DMSO vehicle control was explicitly included to rule out solvent-induced cytotoxicity.

Quantitative Real-Time PCR (qRT-PCR)

To understand the molecular mechanisms driving the physical observations, total RNA was extracted directly from the treated biofilm cells adhered to the microtiter plates (rather than planktonic cells) to accurately capture the biofilm-specific transcriptomic response after 24 hours. Following cDNA synthesis, qRT-PCR was performed targeting a comprehensive panel of five critical genes: *fimH* and *mrkA* (adhesion), *rmpA* and *wzi* (capsule regulation and assembly), and *luxS* (quorum sensing). The 16S rRNA gene served as the internal reference. Its stability under botanical stress was verified, and the results were further validated against *rpoB* as a secondary housekeeping gene. Relative fold changes were calculated using the $2^{-\Delta\Delta Ct}$ method (Harshitha & Arunraj, 2021).

Statistical analysis

All experiments were performed in three independent biological replicates, with each containing technical triplicates. The error bars presented in all figures represent the Standard Error of the Mean (SEM). Data were analyzed using GraphPad Prism software (version 10). Differences between treatment groups were assessed using one-way analysis of variance (ANOVA) followed by Tukey's post hoc test. Statistical significance was set at $p < 0.05$.

Results

Clinical Prevalence and Biofilm Phenotypes

From the initial pool of clinical urine specimens, we successfully recovered and molecularly authenticated 68 *K. pneumoniae* isolates. The primary screening revealed a remarkably high propensity for biofilm formation within this cohort. As illustrated in Figure 1, 80.9% of the isolates exhibited the capacity to form biofilms. More importantly, approximately 60% of these biofilm-producing strains were classified as strong or moderate producers, indicating a high level of structural virulence among the circulating clinical strains. We selected the most resilient isolate from this group for all subsequent functional assays.

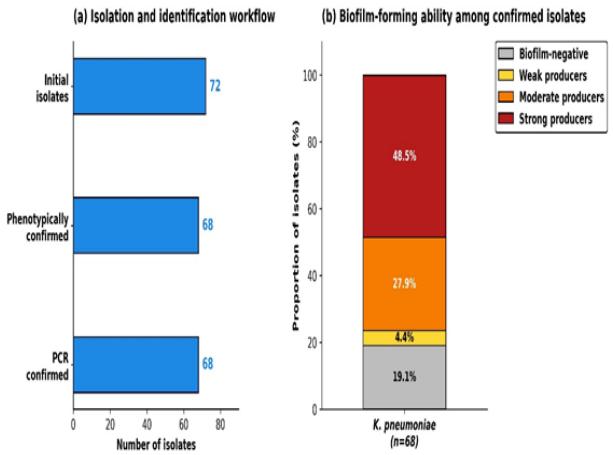

Fig. 1. Phenotypic distribution and biofilm-forming capacity of the recovered *K. pneumoniae* clinical isolates.

Antimicrobial Efficacy and MIC Determination

Before evaluating the anti-virulence properties, we established the direct inhibitory thresholds of the two extracts (Figure 2). The *M. nodiflorum* aqueous extract demonstrated a notably stronger antimicrobial capacity, inhibiting the visible growth of the hyper-virulent *K. pneumoniae* isolate at an MIC of 256 µg/mL. In contrast, the *M. pomifera* extract required twice that concentration to achieve the same bacteriostatic effect (MIC = 512 µg/mL). Based on these metrics, we strictly utilized the respective half-MICs (128 µg/mL for *M. nodiflorum* and 256 µg/mL for *M. pomifera*) for all downstream assays.

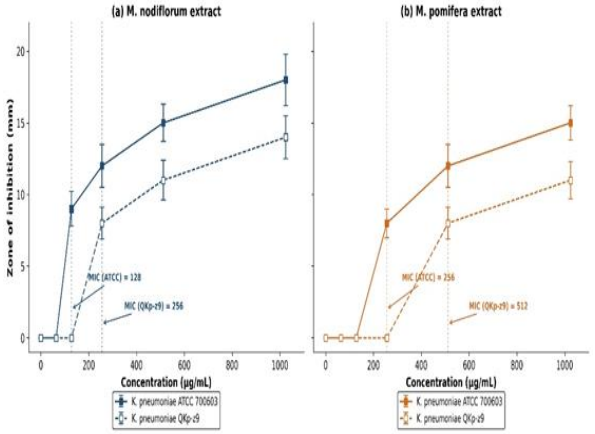

Fig. 2. Minimum Inhibitory Concentration (MIC) and zone of inhibition trends for *M. nodiflorum* and *M. pomifera* extracts.

Sub-Inhibitory Eradication of Biofilm Biomass

Treating the established K. pneumoniae biofilms with sub-inhibitory doses revealed a clear divergence in their disruptive capabilities (Figure 3). Exposure to the ½ MIC of the M. nodiflorum extract severely compromised the biofilm matrix, resulting in a substantial 41.7% reduction in total adherent biomass compared to the untreated controls. On the other hand, the M. pomifera extract struggled to penetrate the extracellular polymeric substance (EPS), managing only a 22.5% reduction in biofilm density. To evaluate dose-dependency, treatments were also performed at ¼ MIC and ⅛ MIC levels, which demonstrated a proportional and significant decrease in antibiofilm efficacy, confirming the dose-dependent nature of the extracts' anti-virulence activity.

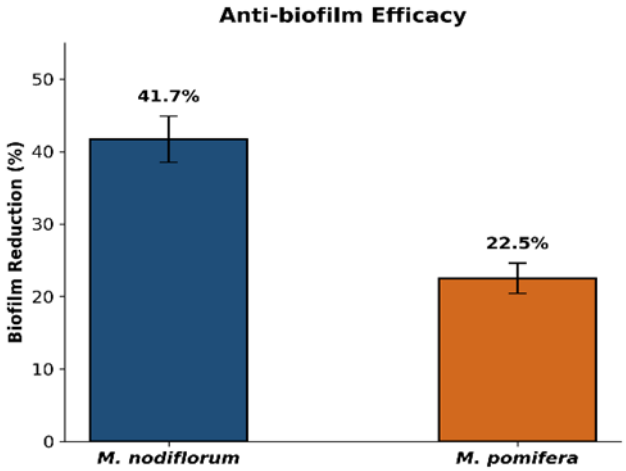

Fig. 3. Anti-biofilm efficacy. Reduction of mature *K. pneumoniae* biofilm biomass following treatment with plant extracts at ½ MIC.

Protective Efficacy in the HK-2 Infection Model

Translating these structural observations to a cellular context, we evaluated how the extracts altered the physical interaction between the pathogen and human kidney epithelial cells (Figure 4). Co-incubation with the M. nodiflorum extract effectively blocked bacterial docking, reducing host cell adhesion by approximately 45%. This protection extended to the intracellular environment, where invasion rates dropped by 40%. The M. pomifera extract, reflecting its weaker anti-biofilm performance, offered significantly less protection, reducing bacterial attachment by only 24% and intracellular invasion by 20%.

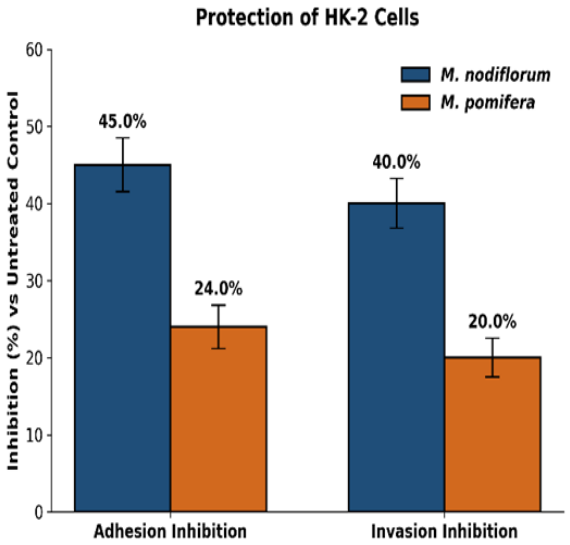

Fig. 4. Protection of HK-2 cells. Percentage of inhibition of bacterial adhesion and intracellular invasion compared to untreated controls.

Host Cell Viability (Cytotoxicity)

Ensuring that the observed reductions in bacterial adhesion were not artifacts of host cell death was a critical prerequisite. The MTT assay confirmed the safety profiles of both botanical interventions (Figure 5). Following a 24-hour exposure, the sub-inhibitory doses of *M. nodiflorum* (128 µg/mL) and *M. pomifera* (256 µg/mL) maintained exceptional cytocompatibility, yielding relative host cell viabilities of 91.4% and 89.2%, respectively.

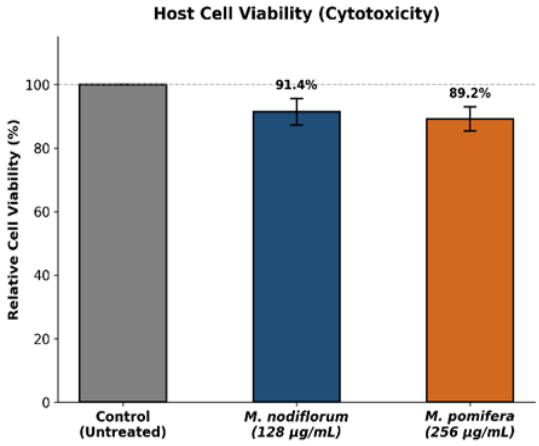

Fig. 5. Host Cell Viability (Cytotoxicity). Relative viability of HK-2 epithelial cells treated with sub-inhibitory concentrations of the extracts.

Transcriptional Repression of the Biofilm Virulence Axis

To uncover the genetic basis for why *M. nodiflorum* outperformed *M. pomifera*, we quantified the expression of five critical virulence genes using qRT-PCR (Figure 6). The transcriptional landscape perfectly mirrored the physical results. *M. nodiflorum* induced a profound silencing across the entire network. It severely repressed the early adhesion machinery, dropping *fimH* and *mrkA* expression by approximately 60% and 45%, respectively. Furthermore, it efficiently shut down the quorum-sensing engine (*luxS*) by 55%, while halving the expression of the capsular assembly genes (*rmpA* and *wzi*). Conversely, *M. pomifera* exerted weak regulatory pressure. While it marginally downregulated *fimH* and *luxS*, it largely failed to disrupt the capsular assembly pathway, leaving the expression of *rmpA* and *wzi* nearly intact.

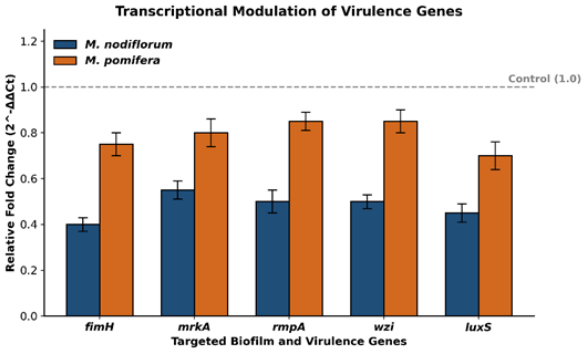

Fig. 6. Transcriptional modulation. Relative fold change in the expression of key biofilm and virulence genes (*fimH, mrkA, rmpA, wzi, luxS*) evaluated by qRT-PCR.

Discussion

The persistent ability of *K. pneumoniae* to form resilient biofilms in the urinary tract represents a formidable clinical challenge (Joseph et al., 2024). Our investigation aimed to evaluate two distinct botanical extracts; *M. nodiflorum* and *M. pomifera*; as potential anti-virulence therapies capable of disarming this pathogen.

Looking at the clinical baseline, our screening revealed that a staggering 80.9% of the recovered isolates were capable of forming biofilms. This high prevalence deeply aligns with recent epidemiological surveys conducted across various provinces in Iran. Several contemporary studies from major Iranian referral hospitals have warned

about a sharp phenotypic shift in uropathogenic *K. pneumoniae*, reporting biofilm formation rates frequently exceeding 75% (Seifi et al., 2016; Hamidi Hesari et al., 2023). This structural resilience explains why conventional therapies are increasingly failing, underscoring the urgent need for alternative anti-biofilm agents (Li & Ni, 2023). When evaluating the anti-biofilm capacities of the extracts, a fascinating divergence emerged. *M. nodiflorum* exhibited marked superiority, reducing mature biofilm biomass by nearly 42% at sub-inhibitory concentrations. In the context of Iranian ethnopharmacology, researchers have extensively explored indigenous flora for their ability to combat Gram-negative biofilms (Qasemi, 2024; Hosseini-nejad & Alimadadi, 2025). The robust performance of the ice plant extract suggests its specific phytochemical matrix is uniquely capable of penetrating the thick EPS of the *Klebsiella* isolates circulating in our region. In contrast, the *M. pomifera* extract only achieved a marginal 22.5% reduction. While previous literature highlights the antioxidant properties of Osage orange, our data indicate that its profile lacks the targeted penetrance required to destabilize the complex architectural shield of *K. pneumoniae* (Pinto et al., 2025; Ampofo et al., 2020).

Validating anti-pathogenic efficacy on human cell lines is a crucial standard to rule out generalized cytotoxicity (Zipperer & Kretschmer, 2017). Strikingly, *M. nodiflorum* almost halved the pathogen's ability to adhere to and invade the HK-2 renal cells, doing so perfectly within a safe, non-toxic therapeutic window (viability >91%). The *M. pomifera* extract offered functionally inferior protection to the host epithelium (Gordon et al., 2018).

What truly sets this study apart is the molecular explanation behind these divergent phenotypes. The qRT-PCR data completely demystify the physical observations (Hampton et al., 2025). *M. nodiflorum* induced a comprehensive transcriptional shutdown of the bacterial offensive network (Herbert et al., 2021). By severely repressing *fimH* and *mrkA*, it essentially stripped the pathogen of its primary attachment tools. Since comparative growth curve analyses confirmed no significant reduction in the cellular growth rate at ½ MIC, the downregulation of adhesion genes reflects a targeted anti-virulence mechanism rather than a secondary artifact of generalized metabolic stress. Furthermore, its ability to halve the expression of *rmpA* and *wzi* reveals exactly how it compromised the biofilm structure: by paralyzing the assembly of the protective capsule (Sahu et al., 2025). This profound genetic suppression was phenotypically validated via a standard "string test," which confirmed a dramatic reduction in the hypermucoviscosity of the *M. nodiflorum*-treated cells. In parallel, the suppression of *luxS* disabled the bacterial communication necessary for biofilm maturation. In *K. pneumoniae*, the *luxS*-encoded AI-2 signaling pathway acts as an upstream master regulator; its suppression directly limits the intracellular signaling cascade required for the optimal expression of fimbrial operons (*fimH/mrkA*). Furthermore, given the prolonged suppression observed, it is highly plausible that this downregulation is not merely a rapid transcriptional response but may involve epigenetic modulations, such as altered DNA methylation patterns within the promoter regions of these virulence genes. On the other hand, the failure of *M. pomifera* was rooted in its inability to exert regulatory pressure on the capsular assembly genes (*rmpA* and *wzi*). The failure of *M. pomifera* to downregulate capsular genes may be attributed to the larger molecular size of its constituent prenylated isoflavones, which likely impedes their penetration through the dense EPS layer to reach their intracellular transcriptional targets. Recent molecular pathogenesis studies have demonstrated that without suppressing the capsular machinery and the *luxS* quorum-sensing engine, dispersing a mature *K. pneumoniae* biofilm is nearly impossible (Chen et al., 2020).

5. Conclusion

This comparative study provides compelling evidence that not all botanical extracts possess the

specific biochemical traits necessary to combat hyper-virulent uropathogens. While *M. pomifera* demonstrated weak anti-virulence properties, the *M. nodiflorum* aqueous extract proved to be a highly potent disruptor of *K. pneumoniae* pathogenesis. By simultaneously dismantling the physical biofilm architecture, protecting human renal tissue from invasion, and molecularly silencing a comprehensive network of fimbrial and capsular genes, *M. nodiflorum* emerges as a highly promising candidate for adjunctive UTI therapies. Moving forward, future research directions must prioritize the bioassay-guided fractionation and chromatographic isolation of the exact active compound(s) responsible for this observed transcriptional repression.However, while these in vitro results are highly encouraging, extensive in vivo validation using animal models is imperative to confirm the bioavailability and clinical translatability of this promising scaffold.

Acknowledgment

The author gratefully appreciate the University of Sistan and Baluchestan for financial support of this research.

Conflict of Interest

The authors declare no conflict of interest.

References

Abhinand, K., Menon, A. M., Thomas, S. S., et al. (2025). Klebsiella pneumoniae: Host interactions, virulence mechanisms, and novel therapeutic strategies. Microbial Pathogenesis, 207, 107856. https://doi.org/10.1016/j.micpath.2025.107856

Ampofo, E. K., Amponsah, I. K., Asante-Kwatia, E., Armah, F. A., Atchoglo, P. K., & Mensah, A. Y. (2020). Indigenous medicinal plants as biofilm inhibitors for the mitigation of antimicrobial resistance. Advances in Pharmacological and Pharmaceutical Sciences, 2020, 8821905. https://doi.org/10.1155/2020/8821905

Arena, R., Manuguerra, S., Collins, E., Mahdhi, A., Renda, G., Messina, C. M., & Santulli, A. (2020). Antioxidant properties of a supercritical fluid extract of the halophyte Mesembryanthemum nodiflorum L. from Sicilian coasts: Nutraceutical and cosmeceutical applications. Applied Sciences, 10(7), 2374. https://doi.org/10.3390/app10072374

Chen, L., Wilksch, J. J., Liu, H., Zhang, X., Torres, V. V. L., Bi, W., Mandela, E., Cao, J., Li, J., Lithgow, T., & Zhou, T. (2020). Investigation of LuxS-mediated quorum sensing in Klebsiella pneumoniae. Journal of Medical Microbiology, 69(3), 402–413. https://doi.org/10.1099/jmm.0.001148

Clinical and Laboratory Standards Institute (CLSI). (2021). Performance standards for antimicrobial susceptibility testing (28th ed., CLSI supplement M100). Wayne, PA: Clinical and Laboratory Standards Institute.

Ding, J., Yan, W., Zheng, R., Ma, M., & Jiang, L. (2025). Combating Klebsiella pneumoniae: From antimicrobial resistance mechanisms to phage-based combination therapies. Frontiers in Cellular and Infection Microbiology, 15, 1691215. https://doi.org/10.3389/fcimb.2025.1691215

Dong, N., Li, R., & Lai, Y. (2022). Editorial: Klebsiella pneumoniae: Antimicrobial resistance, virulence and therapeutic strategies. Frontiers in Cellular and Infection Microbiology, 12, 1108817. https://doi.org/10.3389/fcimb.2022.1108817

Ghasemi, M., Liang, S., Luu, Q. M., & Kempson, I. (2023). The MTT assay: A method for error minimization and interpretation in measuring cytotoxicity and estimating cell viability. In O. Friedrich & D. F. Gilbert (Eds.), Cell Viability Assays. Methods in Molecular Biology (Vol. 2644). New York, NY: Humana. https://doi.org/10.1007/978-1-0716-3052-5_2

Gordon, J. L., Brown, M. A., & Reynolds, M. M. (2018). Cell-based methods for determination of efficacy for candidate therapeutics in the clinical management of cancer. Diseases, 6(4), 85. https://doi.org/10.3390/diseases6040085

Hamidi Hesari, M., Hashemi, T., Hemmat, J., & Sadeghi Fard, N. (2023). Comparison of antibiotic susceptibility of Klebsiella species causing urinary tract infection in Iran and other countries around Asia. Microbiology, Metabolites and Biotechnology, 6(2), 53–62. https://doi.org/10.22104/mmb.2024.6840.1139

Hampton, T. H., Taub, L., Ferreria-Fukutani, K., Stanton, B. A., & MacKenzie, T. A. (2025). Analyzing qPCR data: Better practices to facilitate rigor and reproducibility. Biochemistry and Biophysics Reports, 44, 102356. https://doi.org/10.1016/j.bbrep.2025.102356

Haney, E. F., Trimble, M. J., Cheng, J. T., Vallé, Q., & Hancock, R. E. W. (2018). Critical assessment of methods to quantify biofilm growth and evaluate antibiofilm activity of host defence peptides. Biomolecules, 8(2), 29. https://doi.org/10.3390/biom8020029

Harshitha, R., & Arunraj, D. R. (2021). Real-time quantitative PCR: A tool for absolute and relative quantification. Biochemistry and Molecular Biology Education, 49, 800–812. https://doi.org/10.1002/bmb.21552

Herbert, D. B., Gross, T., Rupp, O., & Becker, A. (2021). Transcriptome analysis reveals major transcriptional changes during regrowth after mowing of red clover (Trifolium pratense). BMC Plant Biology, 21(1), 95. https://doi.org/10.1186/s12870-021-02867-0

Hosseini-nejad, A., & Alimadadi, N. (2025). Antibacterial, anti-biofilm, and antioxidant activities of some Iranian honeys with different floral origins. Iranian Journal of Medical Microbiology, 19(1), 74–82. https://doi.org/10.30699/ijmm.19.1.74

Joseph, B. J., Mathew, M., Rachel, R., Mathew, J., & Radhakrishnan, E. K. (2024). Klebsiella pneumoniae virulence factors and biofilm components: Synthesis, structure, function, and inhibitors. In S. Busi & R. Prasad (Eds.), ESKAPE Pathogens. Singapore: Springer. https://doi.org/10.1007/978-981-99-8799-3_9

Li, Y., & Ni, M. (2023). Regulation of biofilm formation in Klebsiella pneumoniae. Frontiers in Microbiology, 14, 1238482. https://doi.org/10.3389/fmicb.2023.1238482

Mim, T. J., Ahmad, I., Hrach, V. L., et al. (2026). Klebsiella pneumoniae and urinary tract infections: Pathogenesis,

resistance, and advances in management. European Journal of Medical Research. https://doi.org/10.1186/s40001-026-04589-1

Moses, V., Kandi, V., Bharadwaj, V., et al. (2024). Molecular characterization of Klebsiella pneumoniae clinical isolates through whole-genome sequencing: A comprehensive analysis of serotypes, sequence types, and antimicrobial and virulence genes. Cureus, 16(4), e58449. https://doi.org/10.7759/cureus.58449

Pinto, D., Vieira, R., Teixeira, F., Sut, S., Vieira, M., Salazar, M., Delerue-Matos, C., Dall'Acqua, S., & Rodrigues, F. (2025). Unlocking the functional potential of Mesembryanthemum nodiflorum: Insights into digestibility, safety and intestinal uptake. Applied Food Research, 5(2), 101315. https://doi.org/10.1016/j.afres.2025.101315

Qasemi, A. (2024). Comparative effects of Mesembryanthemum nodiflorum extract and biosynthesized silver nanoparticles on the expression of biofilm-related genes in Klebsiella pneumoniae isolated from urinary tract infections in Zahedan (2022–2023). Journal of Epigenetics, 5(2), 53–60.

https://doi.org/10.22111/JEP.2025.50974.1079

Rana, D. S., Sharma, V., & Sheershwal, A. (2025). Understanding host-pathogen interactions in urinary tract infections and advancements in diagnostic methods. Urological Science, 36(2), 61–75. https://doi.org/10.4103/UROS.UROS_98_24

Sahu, A., Jain, S., Junghare, M., Mishra, A., & Ruhal, R. (2025). Biofilm-dispersal patterns in ESKAPE pathogens. Archives of Microbiology, 207(9), 194. https://doi.org/10.1007/s00203-025-04394-0

Sainz-Hernández, J. C., Rueda-Puente, E. O., Cornejo-Ramírez, Y. I., Bernal-Mercado, A. T., González-Ocampo, H. A., & López-Corona, B. E. (2023). Biological application of the allopathic characteristics of the genus Maclura: A review. Plants, 12(19), 3480. https://doi.org/10.3390/plants12193480

Seifi, K., Kazemian, H., Heidari, H., Rezagholizadeh, F., Saee, Y., Shirvani, F., & Houri, H. (2016). Evaluation of biofilm formation among Klebsiella pneumoniae isolates and molecular characterization by ERIC-PCR. Jundishapur Journal of Microbiology, 9(1), e30682. https://doi.org/10.5812/jjm.30682

Stepanović, S., Vuković, D., Hola, V., Di Bonaventura, G., Djukić, S., Cirković, I., et al. (2007). Quantification of biofilm in microtiter plates: Overview of testing conditions and practical recommendations for assessment of biofilm production by staphylococci. APMIS, 115(8), 891–899. https://doi.org/10.1111/j.1600-0463.2007.apm_630.x

Thibeaux, R., Kainiu, M., & Goarant, C. (2020). Biofilm formation and quantification using the 96-microtiter plate. Methods in Molecular Biology, 2134, 183–193. https://doi.org/10.1007/978-1-0716-0467-0_14

Timm, M. R., Russell, S. K., & Hultgren, S. J. (2025). Urinary tract infections: Pathogenesis, host susceptibility and emerging therapeutics. Nature Reviews Microbiology, 23, 72–86. https://doi.org/10.1038/s41579-024-01092-4

Zipperer, A., & Kretschmer, D. (2017). Cytotoxicity assays as predictors of the safety and efficacy of antimicrobial agents. In P. Sass (Ed.), Antibiotics. Methods in Molecular Biology (Vol. 1520). New York, NY: Humana Press. https://doi.org/10.1007/978-1-4939-6634-9_6